

A note on a transverse magnetic field controlled co-current bubble column

Jordan Y. Hristov¹ and Radojica D. Pešić²

¹Department of Chemical Engineering, University of Chemical Technology and Metallurgy, Sofia, Bulgaria

²University of Belgrade, Faculty of Technology and Metallurgy, Department of Chemical Engineering, Belgrade, Serbia

Abstract

An experimental study has been carried out investigating the fluidization behavior of a bubble column with a bottom magnetic particle bed controlled by an external transverse magnetic field. The magnetization-first/gas-scanning mode was applied, at up to 45 kA m^{-1} field intensity, with liquid superficial velocities of up to 20 mm s^{-1} and with a gas flowrate of up to $8 \text{ m}^3 \text{ h}^{-1}$. Particle fractions of two different sizes of up to 1 mm were used. The focus has been both on the three-phase magnetic particle bed expansion playing the role of a gas distributor and the gas holdup of the abovepositioned two-phase section, as well as related column parameters. Piezometric measurements have been performed that provided detection of the position of the interface between the two column sections without visual observation, as well as the gas holdup in the two-phase zone. The bed expansion was strongly affected by the bed state created by the initially established liquid flow rate. The results showed that the intensity of the field applied to the magnetic solids allows control both of bed expansion and internal bed structure, so the applicability of magnetically assisted three-phase bed as a gas distributor in bubble column seems promising.

Keywords: Three-phase magnetic particle bed; bed expansion; gas holdup.

Available on-line at the Journal web address: <http://www.ache.org.rs/HI/>

ORIGINAL SCIENTIFIC PAPER

UDC: 66.096.5:53.082.78

Hem. Ind. 00(0) 000-000 (2024)

1. INTRODUCTION

Process control by application of a magnetic field is a technology for effective regulation of the motion of solids and pertinent heat and mass transfer in fluidized beds (see [1] and the related parts of this series of systematic analyses). Studies on this attractive approach to controlling fluidized beds have been performed applying various field intensities, while most of the reported results have been on gas-fluidized systems due to the simpler design of experimental set-ups than the liquid ones [1]. However, there have been studies on liquid-solid [2] and gas-liquid fluidization [3-7] allowing efficient control of heat and mass transfer processes [8,9].

In the past decade of the 21st century, there have been some studies mainly concentrated on gas and liquid fluidization of admixture of magnetic and non-magnetic particles [10-12], porous electrodes for electrochemical reactors [13,14], pharmaceutical and biotechnological applications [15,16] but reports on three-phase (gas-liquid-solid) beds are practically missing. Moreover, all recent studies mentioned above applied axial magnetic fields (parallel to the column axis and the fluid flow), while studies applying transverse fields are missing.

This article reports experiments on a bubble column, with a bottom bed of ferromagnetic solids, controlled by an external transverse magnetic field. The bed expansion, its role as a gas distributor, gas holdup, and relations of these parameters to existing fluidization regimes are the focus of the study. This report is in tribute to the memory of the late Professor Zeljko Grbavcic, a colleague and friend.

The specific aim of the study refers to the possibility of using a magnetically assisted particle bed as a gas distributor in a bubble column by application of an external (steady state) transverse magnetic field. This solution avoids supporting grids (meshes) or porous plates, commonly used in bubble columns, and allows applications to cases when gases contaminated by fine solids are used. The measurements are focused on the magnetized bed expansion upon conditions

Corresponding authors: Jordan Y. Hristov, Department of Chemical Engineering, University of Chemical Technology and Metallurgy, Sofia, Bulgaria
Paper received: 21 June 2023; Paper accepted: 23 May 2024; Paper published: 24 June 2024.

E-mail: jordan.hristov@mail.bg; jvh@uctm.edu

<https://doi.org/10.2298/HEMIND230621010H>



imposed by the Gas-scanning mode [7], the gas holdup in the two-phase section, and piezometric measurements along the entire column. A specific point coming from the piezometric measurements addresses the detection of the position of the interface between the magnetic bed and the two-phase section.

The application of a transverse magnetic field rather than the common use of axial-oriented ones [7] is motivated by the fact that such an orientation of the field lines allows for avoidance of channeling and the possibility offered by saddle coils magnetic system [1,5,7,8,17] to cover volumes larger than in the case when an axial magnetic field is applied [3,4,5].

It should be noted that bubble sizes and distribution are not considered a topic too common in studies on bubble columns since there was no bubble breakage by floating particle aggregates; such studies in magnetically assisted beds are systematically analyzed in [7,8].

2. EXPERIMENTAL

2. 1. Experimental set-up

The experimental set-up shown in Figure 1 consists of a transparent perplex column (1.95 m in height and 0.1 m inner diameter) with an assigned bottom conical section and a top-located degassing section (conical in shape) containing a droplet separation plate. The bottom section is filled with lead spheres (3 mm in diameter and non-magnetic) playing the role of a static mixer for gas and liquid flows supplied to the upper magnetic section of the column. The magnetic field for controlling fluidization of the ferromagnetic solids was generated by a saddle-coils magnetic system with a maximum field intensity of 45 kA m^{-1} (see more details in [17]). The field orientation, transverse to the column axis and the gas-liquid flow allows efficient control of the motion of the magnetic particles, breakage of the particle aggregates, effective gas bubble breakage (bubble size reduction by mechanical contacts with solids) and avoids channeling. It should be noted that in the case of the axial field *i.e.* parallel to the column axis and particle chains are oriented in the same direction, there is a strong flow bypass through the bed.

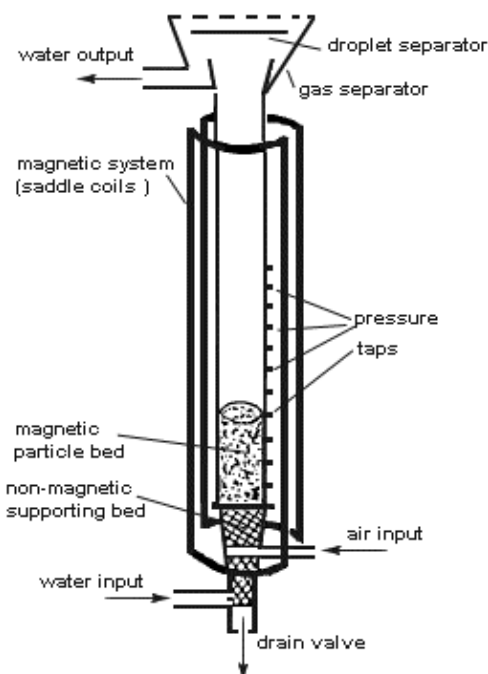


Figure 1. Experimental set-up

A set of vertical glass tube manometers with accessing points (pressure taps) located equidistantly (11 points with a 10 cm distance) along the column was used to measure hydrostatic pressures of the gas-solid-liquid and gas-liquid sections (see the description of the experiment in the sequel), and further used to calculate the gas holdup and solid

phase concentration (controlled by the external magnetic field). A measuring scale mounted along the column for measurement of the bed height and the length of different sections of the fluidized systems was used.

2. 2. Materials used

The experiments were performed with air (supplied by a compressor) and water, at room temperature (20-22 °C) as fluidizing agents. The upper limit of the gas supply flow was about $8 \text{ m}^3 \text{ h}^{-1}$ allowing to study all possible fluidization regimes and measuring the related system parameters. Liquid superficial velocities varied up to 25 mm s^{-1} .

Two sieve fractions of artificial (synthetic) magnetite with alumina doping (Catalyst Haldorf Topsoe, KM-1, Denmark), commonly used for ammonia synthesis, of 0.8 to 1 and 0.3 to 0.4 mm, with a density of 5100 kg m^{-3} were used as magnetic solids. The minimum fluidization velocities concerning the liquid phase were, in the absence of a magnetic field, determined visually from the point where the bed was completely fluidized (almost homogeneous unrestricted motions of all solids through the entire bed volume).

Table 1. Magnetic solids used

Material	Sieve fraction, mm	Density, kg m^{-3}	Magnetization at saturation, kA m^{-1}	$U_{\min} / \text{m s}^{-1}$	
				U_{l0}	U_{g0}
Catalyst Haldorf	0.8 - 1 .0	5100	236.4	0.0203	0.309
Topsoe KM-1	0.3 – 0.4	5100	236.4	0.0038	0.158

U_{\min} - minimum fluidization velocities in the absence of a field; U_{l0} and U_{g0} - minimum fluidization velocities by liquid and by gas

2. 3. Operating modes

The experiments were carried out following the Magnetization-first (corresponding to Fluidization-last) mode [1,7] where the magnetic field is applied on an initially static particle bed, and fluidization starts after that. The fluidization was by the Gas-scanning mode [7], where the liquid flow is established first and then the gas flow is increasing incrementally.

3. CORRELATIONS FOR DETERMINATION OF PHASE HOLDUPS

Here we present the main correlations between the phase holdups in three-phase bubble columns as a base for comparisons and what are the differences when the magnetic particle bed is undergoing fluidization by a gas-liquid flow. Moreover, the focus is on how the piezometric measurements, as a common approach in such studies, can be used to obtain the required information.

3. 1. Conventional relationships for three-phase systems (when a magnetic field is not applied)

From the measurements of the pressure along the column wall, at a given distance h from the magnetic bed base, in the absence of a field, we have Equation (1):

$$P_h - P_{\text{bed-base}} = hg (\rho_s \varepsilon_s + \rho_l \varepsilon_l + \rho_g \varepsilon_g) \quad (1)$$

where h is the distance measured from the bed base, P_h is the pressure, $P_{\text{bed-base}}$ is the pressure at bed base, ε_s , ε_l and ε_g are solids, liquid and gas phase holdups, respectively.

Bearing in mind that the phase holdups are related as in Equation (2):

$$\varepsilon_s + \varepsilon_l + \varepsilon_g = 1 \quad (2)$$

we can define these holdups by Equations (3) to (5):

$$\varepsilon_g = \frac{1}{\rho_l - \rho_g} \left(\rho_l - \frac{\Delta P}{hg} \right) \quad (3)$$

$$\varepsilon_s = \frac{M_{\text{solids}}}{\rho_s h_{\text{bed}} A} \quad (4)$$

$$\varepsilon_l = \frac{1}{\rho_l - \rho_g} \left(\frac{\Delta P}{hg} - \rho_g \right) + \varepsilon_s \frac{\rho_s - \rho_g}{\rho_l - \rho_g} \quad (5)$$



Here, ΔP is the pressure drop between two points at a distance h , M_{solids} is the mass of the magnetic solid phase, A is the cross-section area of the bed (equal to the column cross-section area), and ρ_l and ρ_g are the density of the liquid (water, with $\rho_l = 1000 \text{ kg m}^{-3}$) and gaseous agent (air, with $\rho_g = 1.24 \text{ kg m}^{-3}$), respectively.

3. 2. Specific conditions imposed by the measurement results when a magnetic field is applied

The above Equations (2)-(5) would be valid if the magnetic field does not affect the magnetic bed structure and the particle mobility. In such a case, Equations (2)-(5) are valid and the relation (4) can be used to estimate the initial bed porosity before the magnetic field application. Upon the action of the magnetic field and the induced interparticle forces, we may use only the solid mass M_{solids} conservation relation, Equation (6):

$$M_{\text{solids}} = \rho_s A h_{b0} \varepsilon_{s0} = \rho_s A h_b \varepsilon_s \rightarrow \varepsilon_s = (h_{b0} / h_b) \varepsilon_{s0} \quad (6)$$

where the solid mass in the initial fixed bed is given on the left side of the Equation (6), and the solid mass in the expanded bed is given on the right side of the Equation (6). In Eq. (6) h_{b0} and h_b are the initial bed height and the height of the expanded solids under fluidization conditions, respectively, with the corresponding solid phase holdups, ε_{s0} and ε_s .

Moreover, in such cases, it is impossible to define separately the liquid holdup (ε_l) and gas holdup (ε_g), but only the overall void fraction (*i.e.* overall porosity) ε_{gl} , Equation (7):

$$\varepsilon_{gl} = \varepsilon_g + \varepsilon_l = 1 - \varepsilon_s \quad (7)$$

This is a consequence of the fact that only the solid mass (and volume) remains constant during all regimes of the bed upon fluidization, as expressed by Equation (6).

When the magnetized bed plays the role of a gas distributor and only the two-phase section above it is considered, then Equation (1) can be reformulated as in Equation (8):

$$P_h - P_{\text{bed-top surface}} = hg(\rho_l \varepsilon_l + \rho_g \varepsilon_g) = hg(\rho_l(1-\varepsilon_g) + \rho_g \varepsilon_g) = hg(\rho_l - \varepsilon_g(\rho_l - \rho_g)) \quad (8)$$

Equation (8) indicates a negative slope, almost linear, of the pressure drop profiles along the column wall that could be verified experimentally.

Playing the role of a gas distributor the magnetized bed keeps a fixed structure, resembling a porous medium, and therefore, measurements of the hydraulic pressure drop along its height are proportional to the density of the gas-solid mixtures $\rho_l(1-\varepsilon_g)$ in its free volume without any effects of the solid phase (it is not suspended by the fluid and does not affect the pressure drop measurements). That is, upon the fixed liquid and gas velocities, and field intensity, the pressure drop is determined by Equation (9):

$$P_{h\text{-top}} - P_{\text{bed-base}} = h_b g \rho_l (1-\varepsilon_g) \quad (9)$$

Thus, we may expect almost linear pressure drop profiles along the magnetized bed (see further in section 4.1.).

3. 3. A conjecture pertinent to the detection of the bed top surface

Therefore, to close this point and related explanations, we expect to get from measurements two almost linear pressure drop profiles corresponding to two different physical behaviors of the column sections. Since, the boundary between these sections is the magnetic bed top surface, the conjecture used in this work and experimentally verified is that the linear approximations of these two pressure drop profiles would allow detecting the magnetic bed top surface position even in cases when the column wall is not transparent.

Thus, as follows from the above explanations, the aim was to demonstrate the role of a magnetized bed as a gas-distributor for a two-phase column making such a construction more flexible when dusty gases, for instance, are used, where porous plates, metallic grids, and perforated tubes face problems with clogging, as it was briefly mentioned in section 2. 1. Additionally, studies on bubble breakage by particle aggregates are lacking, while systematic information about hydrodynamic effects are available in [7] and mass transfer related issues are analyzed in [8]. We guess that this remark provides enough additional information so that misinterpretations of the following experimental results are avoided.

4. RESULTS AND DISCUSSION

4. 1. Initial bed expansion in the liquid fluidization mode

The particle bed pressure drop exhibits a strong hysteresis with increases/decreases in the liquid velocity as a sole fluidizing agent. The area of the hysteresis loop depends on the field intensity and is strongly related to the particle aggregations and their field-aligned orientation transverse to the fluid flow (see Figs. 2 and 3). Moreover, the particle strings are induced by magnets, and the repulsive forces between them increase the apparent bed porosity, if the porosity of the aggregates is not considered [1]. This increased free bed volume, allows better gas-liquid mixing with an increased gas flow rate once the gas-scan mode was applied, due to increased bed voids and particle aggregates induce a turbulent fluid flow. The upper limit of the fixed bed defined by the minimum liquid fluidization velocity depends on the field intensity applied, which in general increases as the magnetic field intensity is increased (see Fig. 4). All these preliminary measurements are important to understand the behavior of magnetized solids.

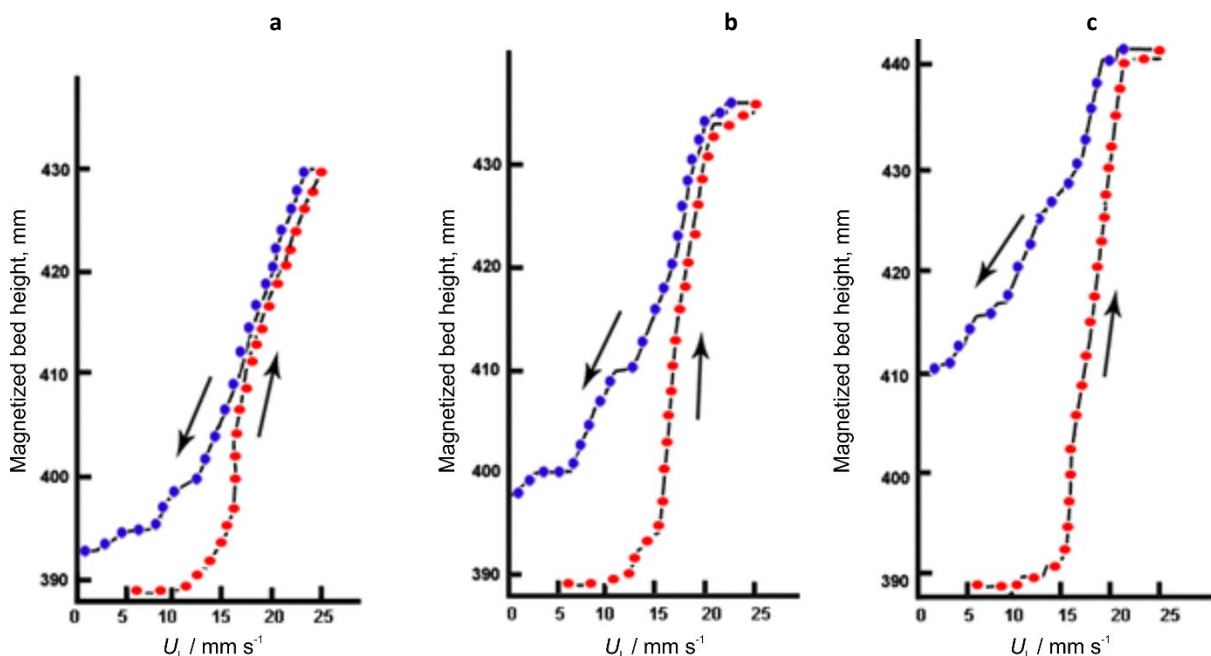


Figure 2. Magnetized bed expansion hysteresis (i.e. bed height) as a function of increasing and decreasing liquid flow at different field intensities: a) $H = 4200 \text{ A m}^{-1}$ b) $H = 8400 \text{ A m}^{-1}$ c) $H = 12600 \text{ A m}^{-1}$. Particle fraction 0.8-1.0 mm

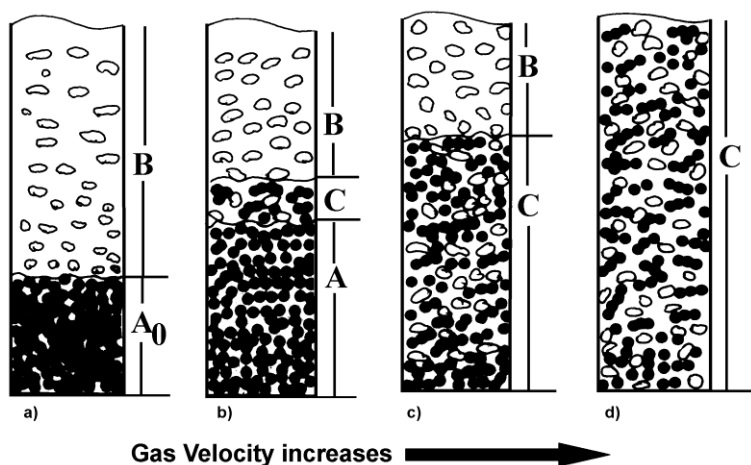


Figure 3. The overall picture of magnetized bed expansion and the definitions of the column sections: a) A_0 - initial fixed bed; b) A - magnetically stabilized bed (MSB); B - two-phase (bubbling) section; C - lean unstable bed at the interface with the two-phase section; c) C - three-phase fully fluidized bed; d) C - complet column three-phase fluidized bed

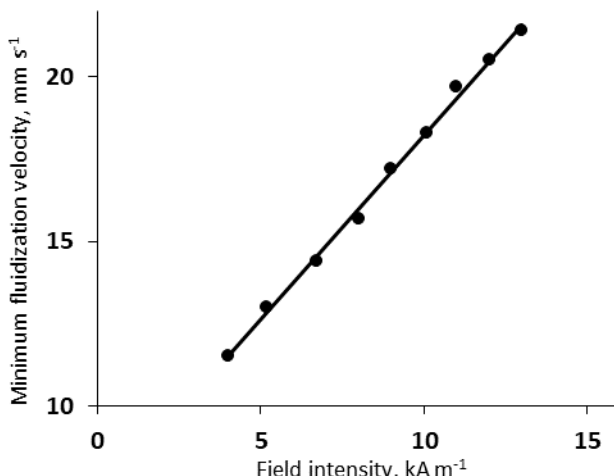


Figure 4. Minimum fluidization velocity concerning the liquid flow as a function of the field intensity applied. Particle fraction 0.8 to 1.0 mm

For the particular case shown in Figure 4, the data could be correlated by a power law, Equation (10):

$$U_{L0} = aH^b \quad (10)$$

The parameters were determined as $a = 1.05 \times 10^{-3} \text{ m}^2 \text{ A}^{-1} \text{ s}^{-1}$, and $b = 6.339$, which is a dimensionless exponent, with $R = 0.9995$, a standard error of 2.007×10^{-6} , estimated by SigmaPlot software (Grafiti LLC, CA). The units of U_{L0} and H are as in Figure 4.

4. 2. Magnetized bed expansion

As can be seen in schematic representation of magnetized bed expansion (Fig. 3), two major sections in the column are distinct at some magnetic field intensity applied. The lower part of the column consists of a three-phase (gas-liquid-solids) section and the upper part of the column consists of a two-phase (gas-liquid) section. Since the upper section is practically similar to the freeboard region in the classic bubble column, the lower section is of particular interest, as different bed structures are established due to the application of gas-liquid flow and the external magnetic field. When the liquid velocity is lower than the minimum liquid fluidization velocity and the gas velocity is lower than the minimum gas fluidization velocity, at some magnetic field intensity, the three-phase section is in the initial fixed (unfluidized) bed regime (Fig. 3a). By increasing the gas velocity, the bed expands slowly, without unrestricted mixing motions of particles, indicating the beginning of stabilization of the bed by the action of the magnetic field. Thus, it demonstrates the well-known behaviour of magnetically stabilized bed (MSB). At some higher gas velocity, on the top of the MSB, there is a small lean unstable three-phase fluidized bed at the interface with the two-phase section (Fig. 3b). The upper limit of MSB is its breakdown at the fluidization onset, *i.e.* minimum gas fluidization velocity. Three phase section become a fully gas-liquid-solid fluidized bed (Fig. 3c). When the gas velocity is high enough, the two-phase section evolves into a complete column three-phase fluidized bed (Fig. 3d).

Upon the simultaneous action of the external magnetic field and the incrementally increasing gas superficial velocity from 0.124 m s^{-1} , the bed expansion (see Figure 5) is strongly affected by the “background” created by the initially established liquid flow rate (below the minimum fluidization point concerning the liquid-solid bed). The plots in Figure 5 correspond to the height of the interface between the the three-phase and the two-phase sections in the magnetized bed (see Fig. 3) *i.e.* each of these lines separates the diagrams in Figs. 5a and 5b into areas. At lower gas velocities the magnetized bed height is constant, so the areas below the bed expansion lines correspond to initial fixed beds at some field intensity applied, while beyond these lines there are bubbling sections. At higher gas velocities magnetized bed height increases with increasing gas velocities and the areas below the bed expansion lines are corresponding to MSBs, while beyond these lines there are fluidized beds where the section A in Fig. 3 disappears and only sections C (fluidized three-phase bed) and section B (two-phase gas-solid section) remain.

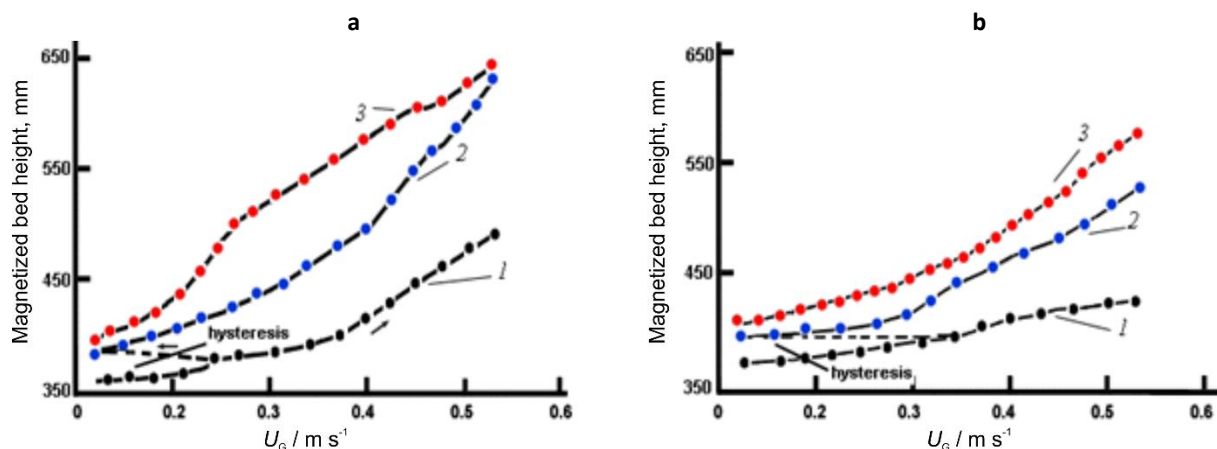


Figure 5. Magnetized bed expansion in the gas-scanning mode at three different liquid velocities (below the minimum fluidization point concerning the liquid-solid bed) and two distinct field intensities: a) $H = 8400 \text{ A m}^{-1}$ and b) $H = 21000 \text{ A m}^{-1}$; liquid superficial velocity: 1 – $U_L = 4.246 \text{ m s}^{-1}$; 2 – $U_L = 10.615 \text{ m s}^{-1}$; 3 – $U_L = 16.982 \text{ m s}^{-1}$; fraction 0.3 – 0.4 mm.

4. 3. Minimum gas fluidization velocity

The minimum gas fluidization velocity of the magnetized solids, in general, decreases with the increase in the liquid velocity (see Fig. 5). The plots in Figure 5 reveal the field intensity effect, that is, increased minimum fluidization velocity as the field intensity is increased, an expected and physically clear effect due to increased interparticle forces and formation of particle aggregates. Besides, with an increase in the magnetic field intensity at a constant liquid velocity below minimum fluidization velocity for liquid solely, the height of liquid-solid bed increases (see Fig. 2) and the liquid holdup increases, the particles are more firmly connected in strings and thus the hydraulic resistance of the bed decreases. This has the consequence that once gas is introduced into the system (gas-scanning mode), a higher gas velocity is required in order to break the fixed structure of the bed thus formed and fluidization to be developed.

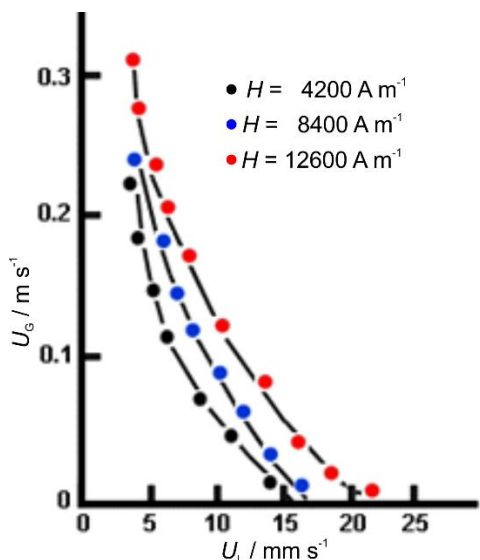


Figure 6. Minimum fluidization velocity concerning the gas flow as a function of the liquid velocity (below the minimum fluidization point concerning the liquid-solid bed) and three intensities of the applied magnetic field. Particle fraction 0.8–1.0 mm

For the plots in Figure 6, the general behaviour of the relationship $U_{G-mf} = f(U_L, H)$ is to a greater extent exponentially decaying and can be presented as:

$$U_{G-mf} = k_H \exp(-bU_L) \quad (11)$$

where the pre-factor k_H and the rate coefficient b depend on the field intensity applied (see Table 2 - data correlation carried out by the software package SigmaPlot).

Table 2. Data correlations of the minimum gas fluidization velocity related to the plots in Figure 6 and correlated by Eq. (11)

$H / \text{kA m}^{-1}$	$k_H / \text{m s}^{-1}$	$b / \text{s m}^{-1}$	Standard error	R
4200	0.4763	0.2163	0.0306	0.901
8400	0.4865	0.170	0.0252	0.923
12600	0.5442	0.448	0.0252	0.923

4.4. Piezometric measurements

Next, the focus was on the data obtained by measurements of the pressure drop profiles along the column axis as commented earlier. This allows us to address: the indirect measurements of the magnetized bed height, the magnetized bed porosity, and the gas holdup in the two-phase section.

4.4.1. Magnetized bed height

The piezometric measurements provide creation of useful pressure drop profiles and comparison of the results thereof with visual bed expansion measurements, precisely the position of the interface separating the three-phase and the two-phase sections of the column. The background used in the data treatment was explained in detail in section 3.

As it is shown in Figure 7 the pressure drop lines change their slopes at the points corresponding to this interface, as suggested by the conjecture in section 3.3. Comparison with the visual observations (see Fig. 8) reveals that there is a satisfactory correspondence between the graphically and the visually determined magnetized bed heights, especially for low and medium field intensities. For the high-field intensity, the discrepancy may reach 10 %. The utility of this result is that piezometric measurements and determination of the specific point of the change in pressure drop slopes allow determination of the interface between the two major zones of the column, even in cases when the column wall is not transparent.

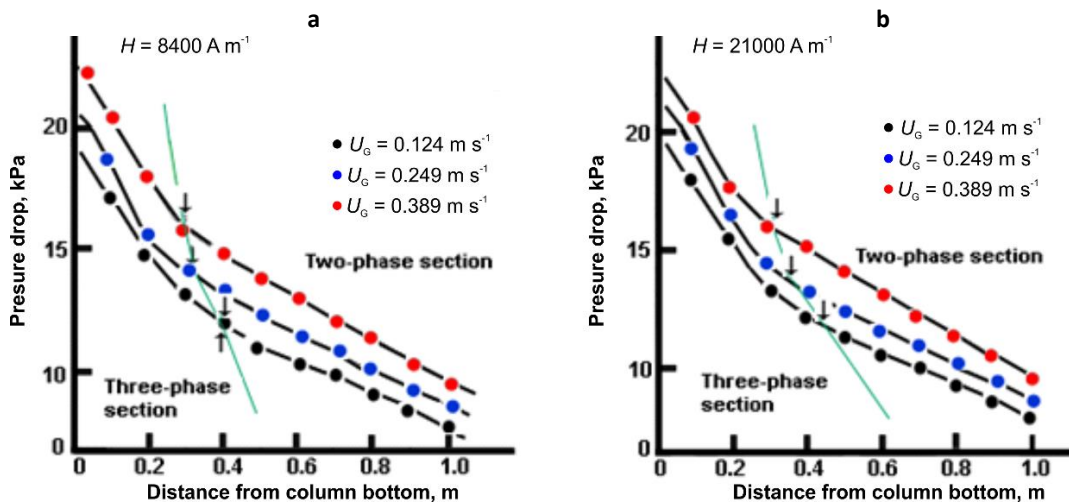


Figure 7. Pressure drop profiles along the vertical column axis determined by the piezometric measurements. The solid lines approximate only the tendency in the pressure drop changes and are not related to any analytic data fittings. The green line shows the points where the pressure drop lines change their slopes, thus indicating the position of the interface B-C (see Fig. 3). Particle fraction 0.8 to 1.0 mm.

4.4.2. Phase holdups

The overall porosity of the magnetized bed (see Fig. 9) increases almost linearly (the approximate green lines) with the gas velocity beyond the minimum fluidization point with a strong effect of the applied field intensity. That is, the stronger the field intensity, the higher the magnetized bed porosity. Since the magnetized bed plays the role of a gas distributor, generating bubbles for the above two-phase section, the increase in the gas velocity yields an increase in the gas holdup, which is an expected result. The measurements, as can be seen from the plots in Figure 10 reveal that the effects of the field intensity are not strong, even though there is a slight increase in ε_g with the increase in the field intensity. This could be attributed to the fact that stronger fields create stronger (stable) magnetic particle structure, and this results in finer gas bubbles generated at the magnetized bed top interface.

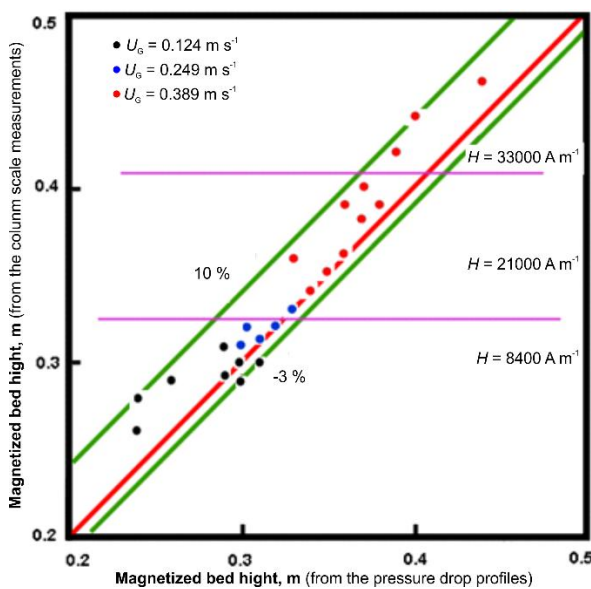


Figure 8. A parity plot between the position of the B-C interface, obtained from pressure drop measurements and the visual measurements at the column wall. Particle fraction 0.8 to 1.0 mm.

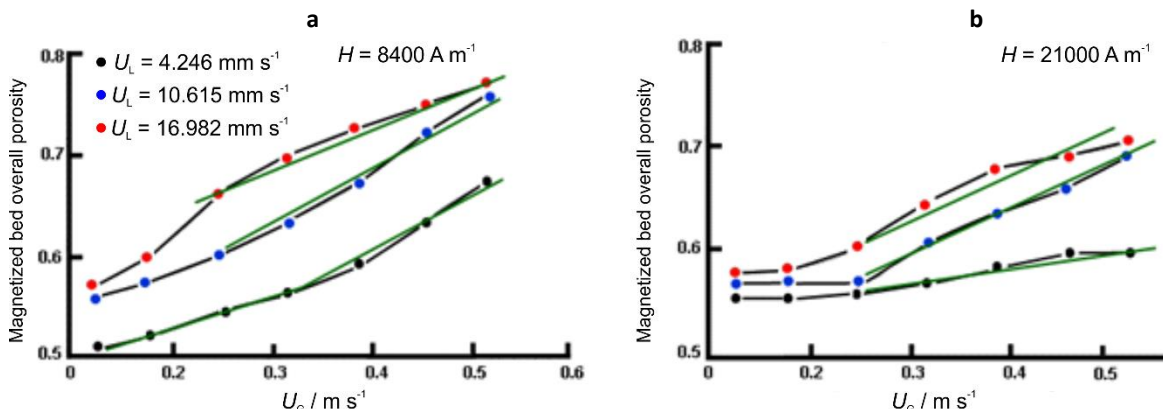


Figure 9. Magnetized bed overall porosity ε_{gi} (combined gas and liquid holdups) as a function of the gas superficial velocity at two distinct intensities of the magnetic field applied. The green solid lines only show almost linear behavior but are not the results of data fittings. Particle fraction 0.3 to 0.4 mm

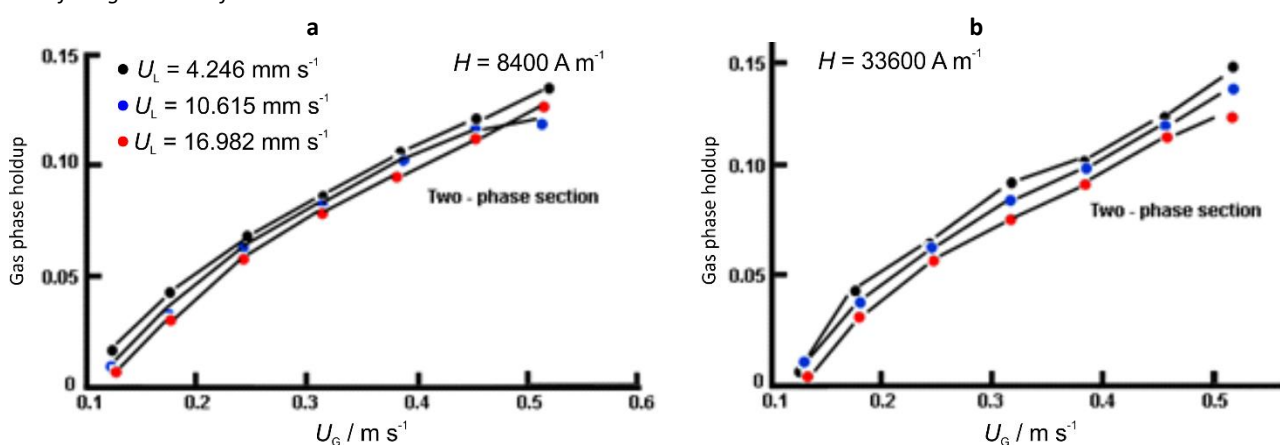


Figure 10. Gas holdup in the two-phase section (when the magnetized bed plays the role of a gas distributor) as a function of the gas velocity. Particle fraction 0.3-0.4 mm.

4. 5. Outlining of the main results

The presented study concerning a bubble column with a magnetized particle bed as a gas distributor is unique even though there are many studies with applications of transverse magnetic fields [1,2,6,7,8,17]. It can be considered as an

upgrade of the research in this field, knowing that there is no literature evidence about three-phase systems under transverse magnetic field.

The main results and contributions can be outlined as follows:

1. It has been demonstrated that a magnetic particle bed can be used as a gas distributor with a structure preliminarily determined by the simultaneous action of both the applied magnetic field and the liquid velocity,
2. The magnetic field intensity allows control of the interparticle forces, thus the bed internal structure and the hydraulic resistance are under remote control,
3. Successful applications of piezometric measurements taking into account the specific conditions due to the imposed magnetic field allowed to create an approach to detect the position of the interface between the magnetized bed and the two-phase section.

5. CONCLUSIONS

This note presented experimental results on a bubble column with a bottom-placed bed of magnetic solids, controlled by an external magnetic field oriented transversely to the column axis. The field orientation and the magnetic system design as saddle coils allow an extended zone of the magnetic bed expansion and control of the bubbles generated at its surface and consequently the gas holdup in the two-phase section above. The pressure drop curves taken from piezometric measurements allowed us to determine the phase holdups in both in the three-phase and two-phase sections as well as the position of the interface between them. The obtained results and the used approach indicate potential benefits for wider applications of transverse magnetic fields in three-phase systems.

NOMENCLATURE

A / m^2	Cross-sectional area of the bed
$b / s m^{-1}$	Rate coefficient in Eq. (11)
$g / m s^{-2}$	Gravity acceleration
h / m	Distance from the magnetic bed base
h_{b0} / m	Initial bed height upon the action of the magnetic field
h_b / m	Expanded bed height upon the action of the magnetic field
$H / A m^{-1}$	Magnetic field intensity
k_H / ms^{-1}	Pre-factor in Eq. (12)
M_s / Am^{-1}	Magnetization at saturation
M_{solids} / kg	Mass of magnetic solid phase
P_h / Pa	Pressure at distance h
P_{h-top} / Pa	Pressure at the top of the bubble column
$P_{bed-base} / Pa$	Pressure at bed base
$P_{bed-top surface} / Pa$	Pressure at bed top surface
$U_G / m s^{-1}$	Gas superficial velocity
$U_L / m s^{-1}$	Liquid superficial velocity
$U_{G-mf} / m s^{-1}$	Gas superficial minimum fluidization velocity in the presence of a magnetic field

GREEK LETTERS

ε_g	Gas phase holdup
ε_l	Liquid phase holdup
ε_{gl}	Magnetized bed overall porosity
ε_s	Solid phase holdup
ε_{s0}	Solid phase holdup in initial bed
$\Delta P / Pa$	Pressure drop between two points;
$\rho_g / kg m^{-3}$	Density of the gas phase
$\rho_l / kg m^{-3}$	Density of the liquid phase
$\rho_s / kg m^{-3}$	Density of the solid phase

REFERENCES

- [1] Hristov JY. Magnetic field assisted fluidization-A unified approach. Part 1. Fundamentals and relevant hydrodynamics. *Rev Chem Eng.* 2002; 18: 295-509. <https://doi.org/10.1515/REVCE.2002.18.4-5.295>
- [2] Hristov JY. Magnetic field assisted fluidization-A unified approach. Part5. A Hydrodynamic Treatise on Liquid-solid fluidized beds. *Rev Chem Eng.* 2006; 22: 195-375. <https://doi.org/10.1515/REVCE.2006.22.4-5.195>
- [3] Sajc L, Jovanovic Z, Vunjak-Novakovic G, Jovanovic G, Pesic R, Vucovic D. Liquid dispersions in a magnetically stabilized fluidized bed (MSFB). *Trans Ichem E.* 1994; 72: 236-240.
- [4] Sajc L, Pesic R, Bursac P, Vunjak-Novakovic G, Bugarski B, Vukovic D. Liquid dispersion in a magnetically stabilized two and three-phase fluidized bed bioreactors. In: *Fluidization VIII: Proceedings of the Eighth Engineering Foundation Conference on Fluidization*. Tours, France, 1995, pp. 425-432.
- [5] Sajc L, Jovanovic G, Jovanovic, Z, Bugarski B. Liquid dispersions in a magnetically stabilized fluidized bed (MSFB). In: Cheremisinoff NP. ed. *Encyclopedia of Fluid Mechanics*, Houston, TX: Gulf Publishing Company.1996, pp. 713-740.
- [6] Hristov JY, Hadzisavas K. Gas-liquid-magnetic solid beds: A classification of the operating modes and a hydrodynamic study in a transverse magnetic field. In: *Proceedings of 2nd European Conference on Fluidization*. Bilbao, Spain, 1997, pp. 565-572.
- [7] Hristov JY. Magnetic field assisted fluidization - A unified approach. Part 6. Topics of Gas-Liquid-solid Fluidized bed Hydrodynamics. *Rev Chem Eng.* 2007; 23: 373-526. <https://doi.org/10.1515/REVCE.2007.23.6.373>
- [8] Hristov JY. Magnetic field assisted fluidization - A unified approach. Part 7. Mass Transfer: Chemical reactors, basic studies and practical implementations thereof. *Rev Chem Eng.* 2009; 25: 1-254. <https://doi.org/10.1515/REVCE.2009.25.1-2-3.1>
- [9] Hristov JY. Magnetic field assisted fluidization - a unified approach. Part 8. Mass transfer: magnetically assisted bioprocesses. *Rev Chem Eng.* 2010; 26: 55-128. <https://doi.org/10.1515/REVCE.2010>
- [10] Zhu Q, Huang Q, Yang C. Hydrodynamic review on liquid–solid magnetized fluidized bed. *Rev Chem Eng.* 2020; 37: 827-861. <https://doi.org/10.1515/revce-2019-0033>
- [11] Zhu Q, Li H, Zhu Q, Li J, Zou Z. Hydrodynamic study on magnetized fluidized beds with Geldart-B magnetizable particles. *Pow Tech.* 2014; 277: 269-285. <https://doi.org/10.1016/j.powtec.2014.08.019>
- [12] Zhu Q, Hao W, Liang P. Magnetic intensification of mass transfer between fluidizing gas and Geldart-B nonmagnetizable particles: Property effects of added magnetizable particles. *Chem Eng Res Des.* 2021; 175: 25-36. <https://doi.org/10.1016/j.cherd.2021.08.034>
- [13] Tschöpe A, Franzreb M. Influence of non-conducting suspended solids onto the efficiency of electrochemical reactors using fluidized bed electrodes. *Chem Eng J.* 2022; 424: 130322. <https://doi.org/10.1016/j.cej.2021.130322>
- [14] Klaiber M, Tschöpe A, Cu K, Waibel I, Heißler S, Franzreb M, Joerg Lahann J. Multifunctional Core–Shell Particle Electrodes for Application in Fluidized Bed Reactors. *ACS Appl Eng Mater.* 2023; 1: 325–333. <https://doi.org/10.1021/acsaenm.2c00072>
- [15] Rakoczy R, Kordas M, Markowska-Szczupak A, Konopacki M, Augustyniak A, Jabłońska J, Paszkiewicz O, Dubrowska K, Story G, Story A, Zietarska K, Sołoducha D, Borowski T, Roszak M, Grygorzewicz B, Dołęgowska B. Studies of a mixing process induced by a rotating magnetic field with the application of magnetic particles. *Chem Proc Eng.* 2021; 42: 157–172. <https://doi.org/10.24425/cpe.2021.138922>
- [16] Grygorzewicz B, Rakoczy R, Roszak M, Konopacki M, Kordas M, Piegał A, Serwin N, Cecerska-Heryć E, El Fray M, Dołęgowska B. Rotating Magnetic Field-Assisted Reactor Enhances Mechanisms of Phage Adsorption on Bacterial Cell Surface. *Curr Iss Mol Biol.* 2022; 44: 1316–1325. <https://doi.org/10.3390/cimb4403008>
- [17] Hristov JY. External Loop Airlift with Magnetically Controlled Liquid Circulation. *Pow Tech.* 2005; 149: 180-194. <https://doi.org/10.1016/j.powtec.2004.11.005>



Barbotažna kolona sa istostrujnim fazama u transferzalnom magnetnom polju

Jordan Y. Hristov¹ i Radojica D. Pešić²

¹Katedra za hemijsko inženjerstvo, Tehnološko-metaluški univerzitet u Sofiji, Sofija, Bugarska

²Univerzitet u Beogradu, Tehnološko-metaluški fakultet, Katedra za hemijsko inženjerstvo, Beograd, Srbija

(Naučni rad)

Izvod

U radu je dat prikaz eksperimentalnih rezultata dobijenih u barbotažnoj koloni sa magnetnom čvrstom fazom smeštenom na dnu kolone, kao raspodeljivačem dvofaznog toka gas-tečnost, pod dejstvom poprečnog magnetnog polja. Najpre je obezbeđen protok tečnosti kroz pakovani sloj čestica, zatim je takav sloj podvrgnut dejству magnetnog polja, a na kraju je uspostavljen protok gasa kroz sloj, koji je obezbedio uspostavljanje fluidizovanog sloja čestica. Eksperimenti su izvedeni pri intenzitetima polja do 45 kA m^{-1} , površinskim brzinama tečnosti do 20 mm s^{-1} i protocima gasa do $8 \text{ m}^3 \text{ h}^{-1}$. Korišćene su frakcije čestica dva različita opsega prečnika, do 1 mm. Fokus je bio na ekspanziji trofaznog sloja magnetnih čestica, koji igra ulogu distributora gasa, kao i na zapreminskom udelu gaa u dvofaznoj sekciji kolone koja se nalazi iznad trofaznog sloja, a takođe i na drugim odgovarajućim parametrima sistema. Izvršena piezometarska merenja su pokazala da je na osnovu njih moguće odrediti poziciju granice između dve sekcije u koloni bez vizuelne detekcije te pozicije, kao i određivanje sadržaja gasa u dvofaznoj sekciji kolone. Na ekspanziju sloja snažno je uticalo stanje sloja stvoreno inicijalno uspostavljenim protokom tečnosti. Rezultati su pokazali da intenzitet polja primerjenog na magnetne čestice omogućava kontrolu kako ekspanzije sloja tako i unutrašnje strukture sloja, na osnovu kojih se prepoznaje potencijalna primenljivost magnetno stabilisanog trofaznog sloja kao distributora gasa u barbotažnoj koloni.

Ključne reči: Trofazni magnetno stabilisani sloj; ekspanzija sloja; zapreminski ideo gasa

--